



**AIN SHAMS UNIVERSITY
FACULTY OF ENGINEERING**

Engineering Physics and Mathematics Department

**Solution of the Navier-Stokes Equations for an
Axisymmetric Vortex Breakdown**

A Thesis

Submitted in Partial Fulfillment for the Requirements
of the Degree of Master of Engineering Science in Engineering Physics and
Mathematics

(Engineering Physics and Mathematics)

Submitted By

Mohamed Ahmed Ibrahim Moustafa

B.Sc., Mechanical Engineering

(Mechanical Power)

Helwan University, 2001

Supervised By

Prof. Dr. / TALAT FAWZY YOUSSEF REFAI

Professor of Engineering Mechanics

Faculty of Engineering-Ain Shams University

Prof. Dr. / MOHAMED HUSSEIN SAID ALI

Professor of Mechanical Power Engineering Faculty of

Engineering-Mattaria

and Dean of Faculty of Industrial Education - Helwan University

Dr. / RABAB MOUSTAFA IBRAHIM

Assist. Prof. of Mathematics

Faculty of Engineering-Ain Shams University

Cairo - 2010

ABSTRACT

Vortex breakdown in swirling flows is characterized by an abrupt change in the structure of the nominally axisymmetric core. The main objective of the present thesis is to give the results of theoretical investigations of axisymmetric vortex breakdown, therefore, been solved partial differential equations, which describe the phenomenon.

For this purpose, the finite difference scheme is proposed and investigated theoretically as well as numerically by solving the equations describing the axisymmetric vortex breakdown which called Navier-Stokes equations.

Steady solutions of the Navier-Stokes equations, in terms of velocity and pressure, for breakdown are obtained numerically using the "Artificial Compressibility" technique combined with an "Alternating Direction Implicit" finite-difference scheme. Axisymmetry is assumed and boundary conditions are carefully applied at the boundaries of a large finite region in an axial plane while resolution near the axis is maintained by a coordinate transformation.

Comparing the theoretical results, which are obtained for the same Reynolds numbers based on the free-stream axial velocity and a characteristic core radius, with [Hafez et al 1986] show that a slight difference of 4% and this should be considered within the descent agreement in the comparisons of theory.

Significantly, on one hand, this work shows that the axial velocity near the axis (w axis) decreases with axial length (z) and then back again to increase. Also, it is found that with increasing the value of specified

circumferential velocity (V) increasing in the rate of decrease in axis velocity is happened near the axis as a result of the phenomenon.

On the other hand, the swirl velocity (v) decreases with increasing in (z). Moreover, it's noticed that the rate of decrease is small at the small circumferential velocity (V).

The results agreed with the practical results of others have been offering some curves to clarify this.

Keywords: Numerical Solution of Partial differential equations, Finite difference methods, artificial compressibility technique, vortex breakdown, Navier-Stokes equations.

TABLE OF CONTENTS

ACKNOWLEDGMENT

ABSTRACT

LIST OF FIGURES iii

NOMENCLATURE vii

CHAPTER - 1: INTRODUCTION 1

1.1 Introduction 1

CHAPTER - 2: LITERATURE SURVEY 4

2.1 Introduction 4

2.2 Solutions of the Navier-Stokes Equations 4

2.3 Overview of the Numerical Investigations 13

CHAPTER - 3: PHENOMENA DISCRIPTION AND

NUMERICAL METHODS 15

3.1 Introduction 15

3.2 Swirling Flows 16

3.3 Recirculation Zones 16

3.4 Types of Breakdown 17

3.4.1 Type 0 17

3.4.2 Type 1 18

3.4.3 Type 2 18

3.4.4 Type 3 19

3.4.5 Type 4 19

3.4.6 Type 5 19

3.4.7 Type 6 20

3.5 Axisymmetric or Bubble Breakdown (type 0) 20

3.6 Numerical Computation of Vortex Breakdown 21

3.7 The Need for Numerical Solution 21

3.8 Finite Difference Method 22

3.8.1 Finite Difference Approximation	23
3.9 Artificial Compressibility Technique	25
3.10 The Alternating Direction Implicit Scheme	25
3.11 Staggered Grid	27
CHAPTER - 4: COMPUTATIONAL TECHNIQUE	29
4.1 Introduction	29
4.2 Navier–Stokes Equations	29
4.3 Mathematical Model	31
4.4 Co-ordinate Transformation	35
4.5 Obtaining the Difference Scheme	37
4.6 Program Validation	53
4.7 Results and Discussion	55
4.8 Comparisons with Experiment Work	76
CHAPTER - 5: CONCLUSIONS	90
APPENDICES:	91
Appendix (A): Computer Program for Theoretical Work	92
REFERENCES:	105

LIST OF FIGURES

	Title	Page
Fig. (1.1)	Vortex breakdown over delta wing	2
Fig. (3.1)	Bubble type breakdown (type 0)	18
Fig. (3.2)	Spiral type breakdown (type 2)	18
Fig. (3.3)	Double helix breakdown (type 5)	19
Fig. (3.4)	Bubble breakdown followed by a spiralling tail	21
Fig. (3.5)	The two half – steps	26
Fig. (4.1)	Boundary condition	34
Fig. (4.2)	Staggered grid system	38
Fig. (4.3)	Axial velocity on axis variation against z at $Re = 100$ and $V = 0.9$	54
Fig. (4.4)	Axial velocity on axis variation against z at $Re = 200$ and $V = 0.9$	54
Fig. (4.5)	Axial velocity on axis variation against z at $Re = 100$ and $V = 1$	55
Fig. (4.6)	Swirl velocity variation against z at $Re = 200$ and $V = 0.63$	56
Fig. (4.7)	Axial velocity variation against z at $Re = 200$ and $V = 0.63$	57
Fig. (4.8)	Pressure variation against z at $Re = 200$, $V = 0.63$	58
Fig. (4.9)	Axial velocity on axis variation against z at $Re = 200$, $V = 0.63$	59
Fig. (4.10)	Axial velocity variation against z at $Re = 200$, $V = 0.8$	60
Fig. (4.11)	Swirl velocity variation against z at $Re = 200$, $V = 0.8$	60

Fig. (4.12)	Pressure variation against z at $Re = 200$, $V = 0.8$	61
Fig. (4.13)	Axial velocity on axis variation against z at $Re = 200$, $V = 0.8$	62
Fig. (4.14)	Axial velocity variation against z at $Re = 200$, $V = 0.85$	63
Fig. (4.15)	Swirl velocity variation against z at $Re = 200$, $V = 0.85$	63
Fig. (4.16)	Pressure variation against z at $Re = 200$, $V = 0.85$	64
Fig. (4.17)	Axial velocity on axis variation against z at $Re = 200$, $V = 0.85$	65
Fig. (4.18)	Axial velocity on axis variation against z at $Re = 200$, $V = 0.9$	66
Fig. (4.19)	Swirl velocity variation against z at $Re = 200$, $V = 0.9$	66
Fig. (4.20)	Axial velocity variation against z at $Re = 200$, $V = 0.9$	67
Fig. (4.21)	Pressure variation against z at $Re = 200$, $V = 0.9$	68
Fig. (4.22)	Axial velocity variation against z at $Re = 200$, $V = 1$	69
Fig. (4.23)	Axial velocity on axis variation against z at $Re = 200$, $V = 1$	69
Fig. (4.24)	Swirl velocity variation against z at $Re = 200$, $V = 1$	70
Fig. (4.25)	Pressure variation against z at $Re = 200$, $V = 1$	71
Fig. (4.26)	Axial velocity variation against z at $Re = 200$, $V = 1.1$	72
Fig. (4.27)	Swirl velocity variation against z at $Re = 200$, $V = 1.1$	72
Fig. (4.28)	Pressure variation against z at $Re = 200$, $V = 1.1$	73

Fig. (4.29)	Axial velocity on axis variation against z at $Re = 200$, $V = 1.1$	74
Fig. (4.30)	Axial velocity on axis variation against z at $Re = 100$, $V = 0.9$	75
Fig. (4.31)	Axial velocity on axis variation against z at $Re = 100$, $V = 1.1$	75
Fig. (4.32)	Axial velocity on axis variation against z at $Re = 100$, $V = 1.3$	76
Fig. (4.33)	Swirl angle distribution at $Re=600$ and $V=0.931$	77
Fig. (4.34)	Swirl angle distribution at $Re=600$ and $V=1.073$	78
Fig. (4.35)	Swirl angle distribution at $Re=600$ and $V=1.176$	78
Fig. (4.36)	Swirl angle distribution at $Re=600$ and $V=1.286$	79
Fig. (4.37)	Swirl angle distribution at $Re=600$ and $V=1.467$	79
Fig. (4.38)	Swirl angle distribution at $Re=868$ and $V=0.856$	80
Fig. (4.39)	Swirl angle distribution at $Re=868$ and $V=0.931$	80
Fig. (4.40)	Swirl angle distribution at $Re=868$ and $V=1.073$	81
Fig. (4.41)	Swirl angle distribution at $Re=868$ and $V=1.176$	81
Fig. (4.42)	Swirl angle distribution at $Re=868$ and $V=1.467$	82
Fig. (4.43)	Swirl angle distribution at $Re=1510$ and $V=0.856$	82
Fig. (4.44)	Swirl angle distribution at $Re=1510$ and $V=1.073$	83
Fig. (4.45)	Swirl angle distribution at $Re=1510$ and $V=1.176$	83
Fig. (4.46)	Swirl angle distribution at $Re=1510$ and $V=1.467$	84
Fig. (4.47)	Swirl angle distribution at $Re=1890$ and $V=0.856$	84
Fig. (4.48)	Swirl angle distribution at $Re=1890$ and $V=1.073$	85
Fig. (4.49)	Swirl angle distribution at $Re=1890$ and $V=1.176$	85
Fig. (4.50)	Swirl angle distribution at $Re=1890$ and $V=1.286$	86
Fig. (4.51)	Swirl angle distribution at $Re=1890$ and $V=1.467$	86
Fig. (4.52)	Swirl angle distribution at $Re=2371$ and $V=0.856$	87

Fig. (4.53)	Swirl angle distribution at $Re=2371$ and $V=0.931$	87
Fig. (4.54)	Swirl angle distribution at $Re=2371$ and $V=1.073$	88
Fig. (4.55)	Swirl angle distribution at $Re=2371$ and $V=1.176$	88
Fig. (4.56)	Swirl angle distribution at $Re=2371$ and $V=1.286$	89
Fig. (4.57)	Swirl angle distribution at $Re=2371$ and $V=1.467$	89

ACKNOWLEDGMENT

I would like to express my special thanks to, ***Prof. Dr. Talat Fawzy Youssef Refai***, whose guidance and encouragement made this study possible, and ***Prof. Dr. Mohamed Hussein Said Ali***, for his valuable guidance, continuous help and the facilities made available to me during all time and preparation of this work.

I would also like to thanks ***Dr. Rabab Moustafa Ibrahim*** for her generous advice regarding the numerical formulation of the problem.

I wish to express my thanks to my colleagues ***Eng. Ahmed Moustafa***, ***Eng. Mahmoud Zaki*** and ***Eng. Ahmed Ali*** for their continuous help during this work.

Finally, I am indebted to my parents and my wife for their support, patience and encouragement during my study and my whole life.

CHAPTER - 1

INTRODUCTION

1.1 Introduction

The term vortex breakdown is used to denote the abrupt disorganization of a slender vortex that occurs when a characteristic ratio of swirl to axial velocity components is varied. The defining features of the phenomenon include the very pronounced deceleration of the stream wise flow along the axis of the vortex accompanied by radial divergence of the stream surfaces. The resulting intense axial flow gradients can lead to the formation of an internal stagnation point on the vortex axis, followed by reversed flow in a region of limited axial extent.

The practical importance of vortex breakdown lies mainly in the field of aeronautics. Since drew attention to its occurrence over wings (aircraft) with highly swept leading edges, when such wings were set at large angles of incidence. The phenomenon was subject of both experimental and theoretical studies. A photograph of vortex breakdown over a delta wing is reproduced in Fig. (1.1).

The aim of the present investigation is to study the solution of steady axisymmetric Navier - Stokes equations for vortex breakdown. Mathematicians actually started their investigations by introducing direct techniques such as finite difference methods. Hence, our main consideration in this thesis is direct towards considering the finite difference method for solving the steady axisymmetric Navier - Stokes equations for vortex breakdown.

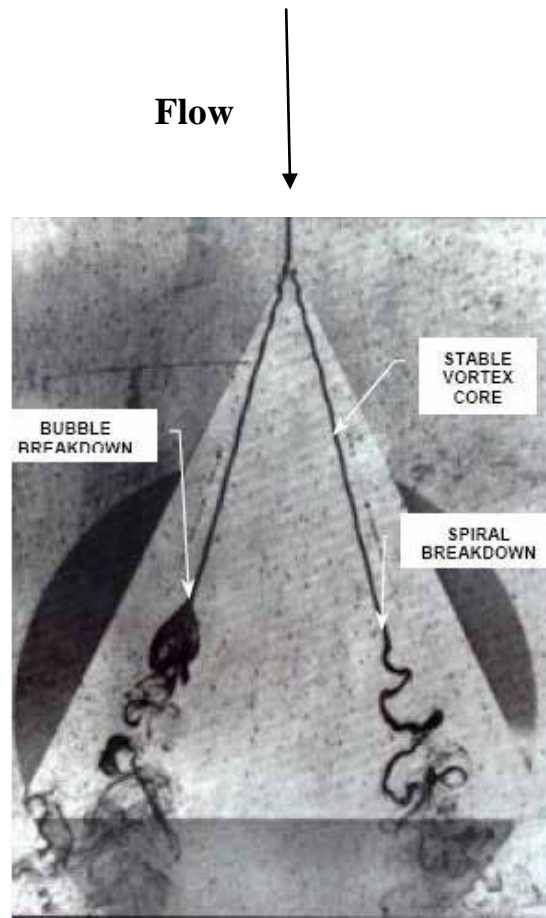


Fig. (1.1) Vortex breakdown over delta wing

The thesis consists of five chapters, two appendices and list of references.

Chapter two is dedicated to give a literature survey of both experimental and numerical investigations for vortex breakdown phenomena introducing by some authors. This chapter ends with the overview of the numerical investigations deduced from the given historical development.

Chapter three starts with a description of the vortex breakdown and different types for it. Focus is put in the finite difference method in solving these equations in this chapter. Chapter three ends with introducing "artificial compressibility" technique to be used in solving the Navier - Stokes equations for vortex breakdown.

The presented work is then included in chapter four which is dedicated to study the mathematical model for vortex breakdown. For this purpose, this chapter starts with displaying the full Navier - Stokes equations. The governing equations of the vortex breakdown are then presented. The chapter marches forward towards introducing the difference schemes used in solving the equations appeared in the mathematical model. The rest of this chapter is dedicated to discussing the effect of different parameters on the results which are confirmed by different charts.

In addition to those chapters, the thesis ends by drawing the main conclusions in chapter five.

Appendix A gives the computer program which has been used to solve the Navier - Stokes equations.

CHAPTER - 2

LITERATURE SURVEY

2.1 Introduction

Vortex breakdown in swirling flows is characterized by an abrupt change in the structure of the nominally axisymmetric core, which gives rise to an internal stagnation point. It represents a crucial element in a variety of technical applications ranging from the stabilization of combustion processes to flows over delta wings. Furthermore, it arises in a number of natural settings such as tornadoes, dust devils and water spouts. In spite of its great importance, a satisfactory understanding of the mechanisms leading to vortex breakdown, and hence the ability to predict it, is still elusive. Hence there is a strong motivation to perform highly accurate, detailed numerical simulations in order to unravel the underlying fluid dynamics.

2.2 Solutions of the Navier-Stokes Equations

The first numerical solutions to the steady axisymmetric equations for vortex breakdown were presented by [**Kopecky and Torrance 1972**]. These were broadly similar, as stated by [**Leibovich 1978**] for a given flow rate, deceleration on the axis and local swelling of the stream lines were obtained at low swirl. At higher values, a stagnation point appeared on the axis followed by a small region of closed streamlines resembling a bubble. Further increasing the swirl caused the bubble to grow in size. The coarser grid used by **Kopecky and Torrance** could be at the origin of this difference. The description seems to agree with some experimental observations. However, a lot of discrepancies:

- The mild bulges obtained at low swirl were never observed experimentally, except as transients. Bubbles smaller than the approaching core radius was also never reported. At low swirl, spiral structures were observed instead.
- Only very slight core expansions were computed, not in relation with the experimental observations.
- The double ring structure observed experimentally in the interior of the bubble by **[Faler and Leibovich 1978]** was not reproduced.

[Shi 1985] presented time-dependent, axisymmetric results which clearly revealed a two-celled structure within the bubble breakdown, together with periodic flow behaviour. He did not report multiple breakdowns. **[Krause and Menne 1987]** also obtained this type of solution when the axial gradient of the radial velocity was set equal to zero in the inflow section ($dv/dx = 0$), instead of assuming an advanced parallel flow ($v = 0$). This type of boundary condition might have been required because of the lack of proper approaching flow. One bubble was first generated containing one vortex ring. Sometimes later, counter-rotating vortex ring appeared. A structure resembling that observed experimentally was obtained for a certain time. However, the structure moved upstream in time and finally reached the inflow cross-section. These initial results seem to show that vortex breakdown could be simulated numerically, provided the vortex structures do not travel upstream to the inflow cross section. However, **[Spall and Gatski 1990]** criticized **[Krause and Menne's 1987]** results as the bubble had lifted off the axis.

Multiple breakdowns have been observed experimentally by **[Harvey 1962]** and **[Sarpkaya 1971]** and have been obtained numerically by **[Hafez**